Jurnal Kejuruteraan 36(5) 2024: 2051–2062
https://doi.org/10.17576/jkukm-2024-36(5)-23

Effect of Multiple Orifices of Wave Energy Converter Air Columns Towards Overall Turbine Output

Nurul Afiqah Mohd Azhar[a], Muhamad Aiman Jalani[a], Mohd Rosdzimin Abdul Rahman[a], Elyasabath Ghazali[c], Mohd Kamarul Huda Samion[c], Yasutaka Imai[d] & Mohd Rashdan Saad[a,b*]

[a]*Centre for Defence Research & Technology (CODRAT),*

National Defence University Malaysia (UPNM),

Kem Perdana Sungai Besi, Kuala Lumpur, 57000, Malaysia

[b]*Department of Aeronautic Engineering & Aviation, Faculty of Engineering,*

National Defence University Malaysia (UPNM),

Kem Perdana Sungai Besi, Kuala Lumpur, 57000, Malaysia

[c]*Hydraulic and Instrumentation Laboratory,*

National Water Research Institute of Malaysia (NAHRIM),

Lot 5377, Jln. Putra Permai, Seri Kembangan, 43300, Selangor, Malaysia

[d]*Institute of Ocean Energy, Saga University, Japan,*

**Corresponding author: mohdrashdan@gmail.com*

Received 28 February 2024, Received in revised form 9 June 2024
Accepted 10 July 2024, Available online 30 September 2024

ABSTRACT

This study investigated a Wave Energy Converter (WEC) device known as the Backward Bent Duct Buoy (BBDB) by looking at the correlation between the number of orifices toward the power generation efficiency. The BBDB type of WEC has a major potential due to its design simplicity and relatively good performance. However, limited studies have been done regarding the BBDB device compared with other types of WEC, especially on the design of orifices. Thus, the objective of this study was to explore the effect of having a multiple number of orifices on the top panel of the BBDB device toward its power efficiency. It was achieved by designing and fabricating four BBDB top panels with varying number of orifices followed by experimental wave tank tests. The results showed that the top panel with 2 orifices produced the highest efficiency of 39% followed by the top panels with 4 orifices (27%), 1 orifice (23%) and 3 orifices (22%). This leads to the conclusion that top panels with multiple orifices promote better efficiency than single orifice.

Keywords: Ocean energy; renewable energy; Wave Energy Converter (WEC); Oscillating Water Column (OWC); Backward Bent Duct Buoy (BBDB); orifice

INTRODUCTION

Recently, the global demand for energy has been growing due to a large and aggressive rise in human population. This resulted in increased usage and consumption of fossil fuels worldwide, with its highest peak was recorded in 2016 (Dincer et al. 2018). Such a trend raises a prominent concern particularly from the environmental perspective as the burning of fossil fuels and discharging of carbon dioxide contribute toward serious greenhouse emission that is harmful to both human and the environment (Wuebbles & Jain 2001). It also subscribes to the sustainability concern since fossil fuels are considered non-renewable energy with limited sources. Therefore, more calls have been made for other sources of energy that are sustainable and impede minimal to no pollution, such as renewable energy.

One of the most promising renewable energy sources is ocean energy, which refers to types of renewable energy that can be generated from the sea or the ocean. Since 70% of the Earth's surface comprises the ocean, ocean energy is propounded as a highly accessible renewable energy. It also stands as the best basis to generate power as the production is nearly 90% of all time in comparison to 25% for both wind and solar devices. Ocean energy can be categorised into 3 types, which are thermal energy, chemical energy, and mechanical energy. Among the examples of ocean energy include ocean thermal energy conversion (OTEC), tidal energy, and wave energy (Dincer et al. 2018; Fusheng et al. 2016; Aderinto & Li 2018).

OTEC can be generated from the temperature difference between the deep water and the surface of the ocean. Meanwhile, tidal power is one of the oldest energy production methods where the natural rise and fall of the tides is used to generate electricity, which is nearly similar to a hydro-power plant. Finally, wave energy, also known as wave energy converter (WEC), harvests energy from the motions of the wave and converts it into electricity.

Researchers believe that WEC has several advantages compared to other types of ocean energy; the waves provide the highest and most reliable energy density as it is always in motion (Drew et al. 2009; Zhang et al. 2009). There are several types of WEC such as Oscillating Water Column (OWC), point absorber, attenuators, and overtopping (Dolores et al. 2017; Falcao 2009; Lindroth & Leijon 2011; Astariz & Iglesias 2015; Pietra et al. 2012). Among all, OWC has the advantage of having a simple body structure with no moving parts installed at an underwater level, making it easy to access the power take-off unit as it is straightforward (Wu et al. 2018). There are four types of floating OWC, namely Forward Bent Duct Buoy, Backward Bend Duct Buoy (BBDB), Centre Buoy Pipe, and Sloped Buoy. The Backward Bent Duct Buoy (BBDB) and Forward Bent Duct Buoy are low in cost and have a simple single floating structure, whereas the Centre Buoy Pipe and Sloped Buoy use in-depth drafts that require special equipment to be transported in addition to the complicated adjustments, which will consume more time for installation. Moreover, the mooring cost is low since the device can advance the weather by itself (Murakami et al. 2016).

The BBDB is widely utilised as its shallow drafts design enables it to be moved and installed easily. Nevertheless, not many studies have been done regarding BBDB compared with other types of WEC. According to Joubert et al. (2013), only 3 out of 172 types of WEC listed were categorised as BBDB, namely the Ocean Energy (OE) buoy or OE 35, OE Generation Platform or OE 12, and a developing 5kW floating offshore OWC from Guangzhou Institute of Energy Conversion (GIEC). However, both OE 35 and OE 12 were only quarter-scale prototype models. OE buoy has a low environmental impact as the device does not have any open moving parts that can harm the marine life. It is also easy to maintain as the turbines and generators are located outside of the water, which can prevent corrosion and are easily accessible.

An experiment by Howe & Nader (2017) reported that the chamber geometry of an OWC device has a significantly small effect on the performance of the bent duct OWC. The rectangular device provided a more variable design solution when the constructability and marine structure integration were considered. The authors also proposed using an L-shaped duct as an OWC chamber.

Meanwhile, a study on the shape geometry of floating oscillating water columns by Kim et al. (2015) reported that having a rounded corner shape could result in a high-power output than sharp shapes. The result is further supported by Aiman et al. (2020) who stated that having a rounded corner prompted higher primary efficiency at a low value of λ_{Λ} in comparison to other models such as rectangular corner and corner with 45 degrees.

Regarding the front shape of BBDB, the shape model of pentagonal BBDB resulted in a higher primary conversion efficiency (Wu et al. 2017; Li et al. 2019; Wu et al. 2018; Li et al. 2019. Wu et al. (2018) compared three different models and found that pentagonal BBDB had the highest efficiency. Such finding is aligned with Wu et al. (2017), Li et al. (2019) and Li et al. (2019).

According to Imai et al. (2010) and Baanu et al. (2014), extending the duct of BBDB will decrease its primary conversion efficiency. The finding agrees with an experiment conducted by Toyota et al. (2010) where Type A1 (actual length of duct) gave out the highest efficiency compared to Type A2 and Type A3 where the ducts were extended. However, Toyota et al. (2008) ran a test for 5 different types of BBDB body hulls and the results revealed that BBDB with a duct extension recorded the best performance of 0.35 for primary conversion efficiency. The authors believe that such difference in the results might owe to the body shape of the BBDB.

On the other hand, Celik & Altunkaynak (2019) posit that having a higher orifice diameter does not guarantee increased primary conversion efficiency of the BBDB device as there are several parameters and conditions that must be considered including wave height. A study on different buoyancy models by Toyota et al. (2010) showed that having a rectangular with rear semi-cylindrical model resulted in the highest efficiency (95%) than other cylindrical buoyancy models (60% efficiency).

Furthermore, Diaz et al. (2018) experimented with the behaviour of BBDB such as the heave and pitch motions, power output, and pneumatic efficiency. The results demonstrated that wave height has a significant influence on efficiency while the mooring characteristics can affect the device's efficiency. It was also revealed that a mooring that allowed a smaller surge motion would increase the efficiency of the device for regular and random waves. Rezanejad et al. (2017) further reported that the turbine damping coefficient and wave period have a dominant impact on the performance of the device. Their results also confirmed that higher wave height resulted in higher device efficiency in a large wave period; nevertheless, increasing the wave height would boost the device performance in low damping conditions regardless of the wave period.

Past studies have also looked at the aspect of multi-oscillating water column (M-OWC), also known as multichamber oscillating water column (MC-OWC) (Doyle & Aggidis 2019; Doyle & Aggidis 2020; Delmonte et al. 2014). Both M-OWC and MC-OWC comprise 3 categories, which are OWC array, modular M-OWC, and segmented M-OWC. OWC array is a single unit consisting of several OWCs housed in the same structure, each operating independently with its own turbine and generator. Whereas, modular M-OWC has many chambers which provide airflows that are combined, gathered, and possibly modified at the upstream of the turbine. As a result, the various OWC systems are integrated prior to the power take-off (PTO) stage to produce a constant unidirectional airflow. On the other hand, the same generator is operated in segmented M-OWC by mechanically connecting the turbines of various OWCs while remaining segregated. Among the examples of M-OWC include Wave Mill and the LEANCON device. In a study that compared the performance of a single OWC array and M-OWC, Doyle & Aggidis (2020) discovered that M-OWC produced higher flow rates and power compared to the other device. However, when considering the efficiency and the total capture width values, the WEC's efficiency concerning the total capture width decreased as the spacing widened. Nevertheless, no M-OWC studies to date have used multiple orifices for each of the singular OWC. Hence, this research was conducted to address the gap regarding the usage of multiple orifices. To date, most existing studies are focused on how factors like the chamber geometry shape, front shape, corner geometry shape, duct extension, orifice diameter, multi-OWC, buoyancy model, mooring characteristics, and turbine damping coefficient affect the performance of BBDB devices. However, limited studies have looked at the characteristics of orifice, especially focusing on how the number of orifice affects the performance of BBDB devices. As such a gap in knowledge can halt further efforts to improve BBDB devices and its efficacy, this study aims to address the issue by investigating the effect of using single and multiple orifices toward the performance of BBDB devices. It is believed that optimising orifice will result in increased BBDB performance hence contributing to higher efficiencies of wave energy converter devices.

METHODOLOGY

THE DESIGN AND FABRICATION OF BBDB TOP PANEL

SolidWorks CAD software was used in this study to design the BBDB orifice and the top panel dimensions. Figure 1 shows the drawing and dimensions of BBDB from three points of view while Figure 2 shows the top panel design with 1 (baseline), 2, 3, and 4 orifices. The dimension of the top panel with 3 orifices was labelled from left to right while the dimension of the top panel with 4 orifices, each orifice was labelled (1 to 4) accordingly from left to right (see Figure 2). The diameters for the orifice, water level sensors, and pressure sensor were 40 mm, 20 mm, and 10 mm, respectively. The orifice's diameter was determined based on previous studies by Imai et al. (2008), Imai et al. (2010), and Aiman et al. (2020) while the BBDB dimension was adopted from Aiman et al. (2020). Additionally, the top panels of the air columns were fabricated before conducting a wave tank test to measure the primary conversion efficiency, which was done using acrylic sheet materials and a laser cutting method (see Figure 3).

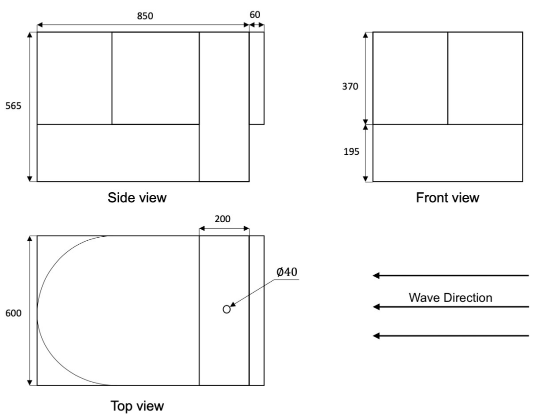

FIGURE 1. Drawing and dimensions of BBDB with 1 orifice. All units are in millimetre(mm)

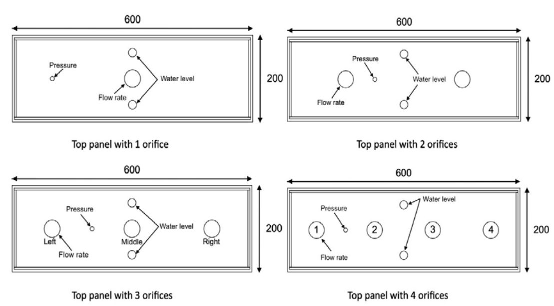

FIGURE 2. Design of the top panels with multiple orifices. All units are in millimeter(mm)

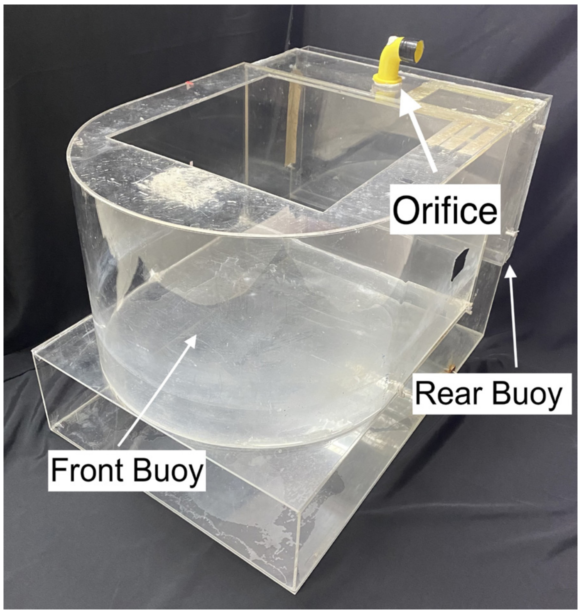

FIGURE 3. Different components of Backward Bent Duct Buoy (BBDB) Device

WAVE FLUME TEST

The experiment was conducted in a 2D wave flume located at the Hydraulic and Instrumentation Laboratory National Water Research Institute of Malaysia (NAHRIM). The laboratory had been used to conduct several other past studies (Aiman et al. 2020; Husain et al. 2019). As shown in the schematic diagram (see Figure 4), the 2D wave flume was 100 m long, 1.5 m wide, 1.2 m deep, and 2 m in height. There was an absorber wall positioned at the downstream of the flume to prevent interaction between waves. Figure 5 presents a view of the 2D wave flume from upstream while Figure 6 shows the top view of the BBDB setup. Additionally, the combination of 0.05 m - 0.10 m wave height and 1 s – 5 s wave period was used in this study to match the low heave wave condition.

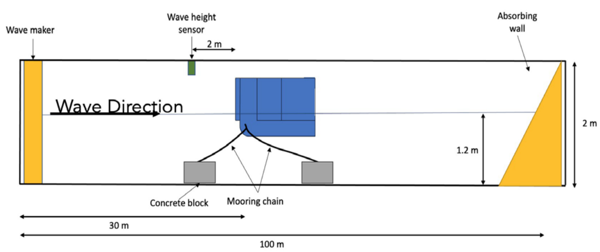

FIGURE 4. Schematic diagram of the experiment setup

FIGURE 5. 2D Wave Flume

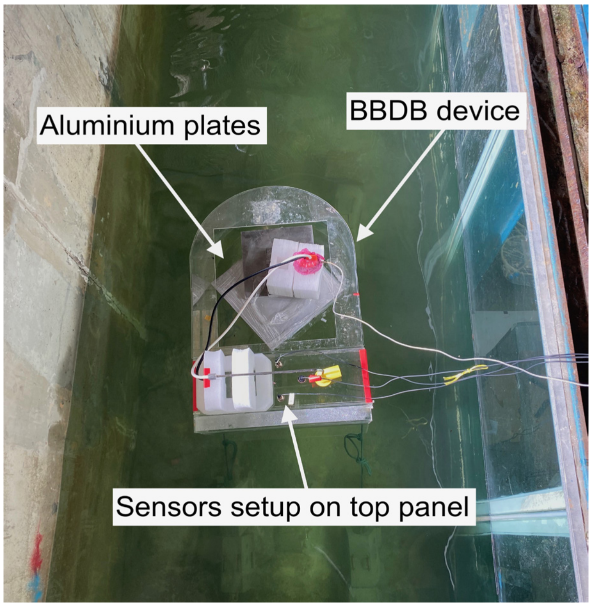

FIGURE 6. Top view of BBDB setup

INSTRUMENTATION

A set of sensors configuration was attached on top of the model (Figure 7) and connected to a set of amplifiers within the instrumentation setup (Figure 8) to amplify data from the sensors. Meanwhile, the flow rate data were collected separately using a pitot tube anemometer (Figure 9).

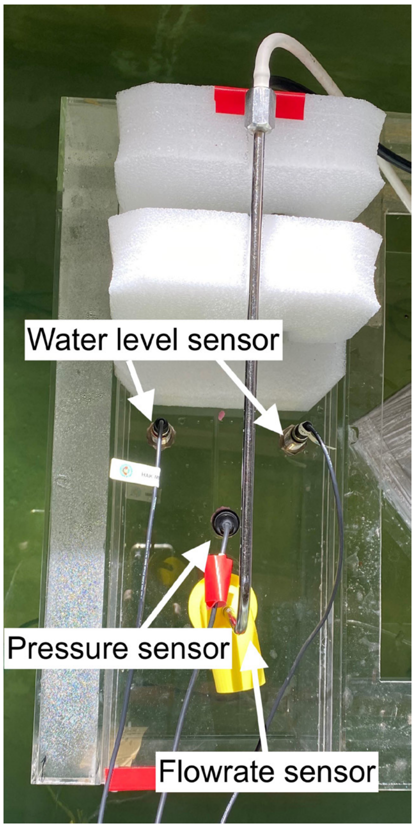

FIGURE 7. Instrumentation setup on board the BBDB model

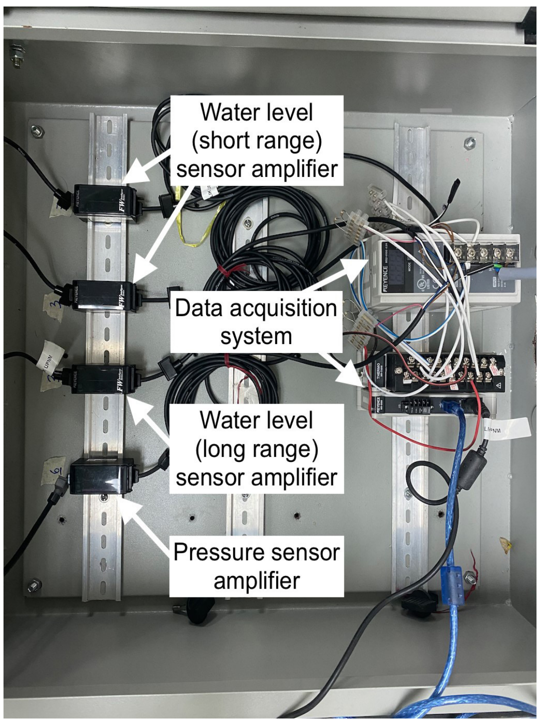

FIGURE 8. Layout of the instrumentation used in experiment

FIGURE 9. Pitot tube anemometer used to measure flow rate

The sensors consisted of two digital ultrasonic water level sensors KEYENCE FW-H07 (±0.001 m accuracy) to measure the water level inside the water column, a pitot tube anemometer EXTECH HD-350 (0.0001 m^3/min accuracy) to measure the flow rate at the orifice, and a KEYENCE AP-10S (0.01 kPa accuracy) air pressure sensor to measure the air pressure inside the water column. All data from the sensors and amplifiers were acquired through the data acquisition system (KEYENCE NR 500) as shown in Figure 10. Finally, the data were visualised in the data acquisition software (KEYENCE Wavelogger). A long-range water level sensor, KEYENCE FW-H10R (±0.001 m accuracy), was placed 2m upstream from the model to measure the height of the incoming wave. This ensured that both wave height output and wave height input were similar. The difference between the wave height output and wave height input was estimated to be within ±0.001 m.

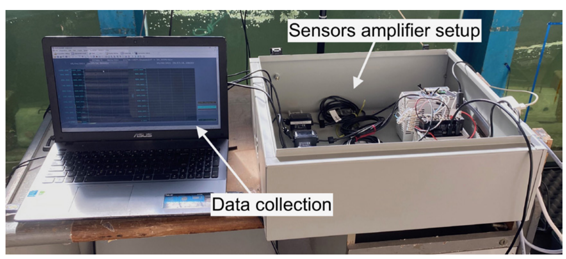

FIGURE 10. Data acquisition setup for all sensors

2 mooring lines were attached to each side of the bottom of the model with concrete blocks tied on the other end of the lines. This was to avoid the BBDB from moving during the experiment. The material used for the mooring line was nylon with a thickness of 12 mm. Nylon is known for its strength, durability, and stretch, and has been used in the marine industry for many years. Catenary mooring system was used in this experiment since it had the shape of a free-hanging line that allowed better movement of the device instead of being fixed in one place. This was crucial because the device had to oscillate in order to optimise the airflow and the power output. An additional weight of 12.5 kg was placed inside the front buoy of the BBDB device to ensure its stability after deployment.

The 2D wave flume and wavemaker were controlled from a control room. Both the wave height and period were set before running the wave test. The wave paddle then oscillated to produce waves for the wave flume. Three different wave heights were used to experiment with 1 orifice, namely 0.05 m, 0.08 m, and 0.1 m. Whereas, only 0.1 m wave height was used to run the experiment for 2, 3, and 4 orifices since it gave the best output.

PRIMARY PERFORMANCES OF OSCILLATING WATER COLUMN

This study calculated the primary conversion efficiency of the BBDB device based on Equation 1, which was adopted from Macfarlane et al. (2017). The BBDB efficiency could never be calculated without wave energy and air energy; thus, it was crucial to calculate the wave energy and air energy produced during the experiment.

$$n_1 = \frac{E_{air}}{E_{wave}} \tag{1}$$

Wave energy refers to the energy gained from incident waves and it was calculated in this study using Equation 2.

$$E_{wave} = \frac{1}{2}\rho g \zeta^2 C_g B \tag{2}$$

where ρ, g, ζ, B, c_g , k, Ω, λ and h are the water density (kg/m^3), the gravitational accelerations (m/s^2), incident wave amplitude (m), width of the OWC device perpendicular to the incident wave direction, the group velocity (m/s), wave number, angular frequency of the wave(rad/s), wavelength (m) and water depth (m) respectively. Group Velocity, c_g is the velocity with which a wave packet travels. The equation is as shown in Equation 3.

$$C_g = \frac{\Omega}{2k}\left(1 + \frac{2kh}{\sinh(2kh)}\right) \tag{3}$$

Meanwhile, wave number. k was the spatial frequency of a wave measured in cycles per unit distance (ordinary wavenumber) or radians per unit distance (angular wavenumber) as shown in Equation 4. In this case, λ was the angular frequency of the wave (rad/s).

$$k = \frac{2\pi}{\lambda} \tag{4}$$

On the other hand, air energy referred to the pneumatic output energy gained from the orifice that was located at the top panel column. Air energy was calculated in this study using Equation 5; however, it was crucial to know the pressure difference output.

$$E_{air} = \frac{1}{T}\Delta P(t)Q(t)dt \tag{5}$$

This equation accounts for the dynamic interaction between pressure difference and flow rate over time, providing an accurate measure of the total work done by the air. In this regard, the pressure difference, ΔP, was determined by subtracting the maximum and minimum pressure gained while Q was the flow rate gained from inside of the water column. Additionally, the calculation for E_{air} of the top panel with 1 orifice is shown in Equation 5 whereas, for 2, 3, and 4 orifices, the E_{air} of each orifice with the same wave height and period were initially summed up before divided with E_{wave} as shown in Equation 6.

$$\Sigma E_{air} = E_{air1} + E_{air2} + \cdots + E_{airn} \tag{6}$$

RESULTS AND DISCUSSION

PRESSURE IN WATER COLUMN

Pressure plays an important role in calculating the efficiency of the BBDB device. According to the formula of air energy in Equation 5, the pressure difference influences the air energy, which then influences the efficiency. Thus, higher pressure difference is better since the efficiency of the device will increase as well.

The amplitude of the inner pressure of the water column for all top panels with the wave height of 0.1 m was plotted in Figure 12. The measurement uncertainty for each data point in Figure 12 estimated using the Extech HD350 pressure sensor accuracy and assuming a repeatability standard deviation of ±0.0002, is approximately ±0.00046. It was observed that the trend for all top panels was slightly similar. In this regard, the top panel with 4 orifices increased gradually from $\lambda_{/L}$ = 2.0 to 5.0; however, it started to drop steeply until $\lambda_{/L}$ = 11.0 and continued to increase again. As for the top panel with 2 orifices, the pressure also increased gradually from $\lambda_{/L}$ = 2.0 to 5.0 before it began to decrease until $\lambda_{/L}$ = 10.0. The results indicate that the trend line for both top panels with 2 and 4 orifices was similar. On the other hand, the top panel with 3 orifices was observed to decrease, slightly increase to $\lambda_{/L}$ = 2.0, before it decreased again until $\lambda_{/L}$ = 11.0. Whereas, the trend line for the top panel with 1 orifice was unstable as it was constantly increasing and decreasing between each point. Hence, no specific trend line was observed for the top panel with 1 orifice.

Further observation revealed that there was a similar trend line when λ/L = 2.0 to 4.0 and λ/L = 15.0 to 20.0. During $\lambda_{/L}$ = 2.0 to 4.0, the pressure increased; whereas in $\lambda_{/L}$ = 15.0 to 20.0, the pressure for all top panels continuously decreased due to the decreasing water elevation. As shown in Figure 12, the top panel with 4 orifices has the highest value of pressure amplitude, P/ρgZi = 4.52. The high pressure difference occurred due to the increase in water elevation. This is because a higher water elevation will decrease the static pressure, hence increasing the pressure difference. As seen in the graph plotted below, the top panel with 4 orifices performed the best by providing the highest pressure difference compared to other top panels. As air exited through the orifices, the mass of air flowing from the 2-orifice configuration created a nozzle effect that produced a higher flow rate compared to the 4-orifices configuration. Such case happened because the 2-orifice top panel had a more focused exit than the 4-orifice top panel, subsequently resulting in higher air flow momentum due to the higher velocity of airflow. This theory is further supported by Golijanek-Jedrzejczyk et al. (2022). The present study concludes that a slight, localised increase in pressure occurs as a result of fluid particles accumulating on the front surface in front of the orifice during the flow. The moving fluid encounters zones of lower pressure and properties that tend to vacuum after passing through the holes, hence creating a chaotic swirl. Thus, having 4 orifices creates a smaller distance between each orifice, subsequently increasing the zone of reduced pressure and causing more chaotic swirls compared to 2 orifices.

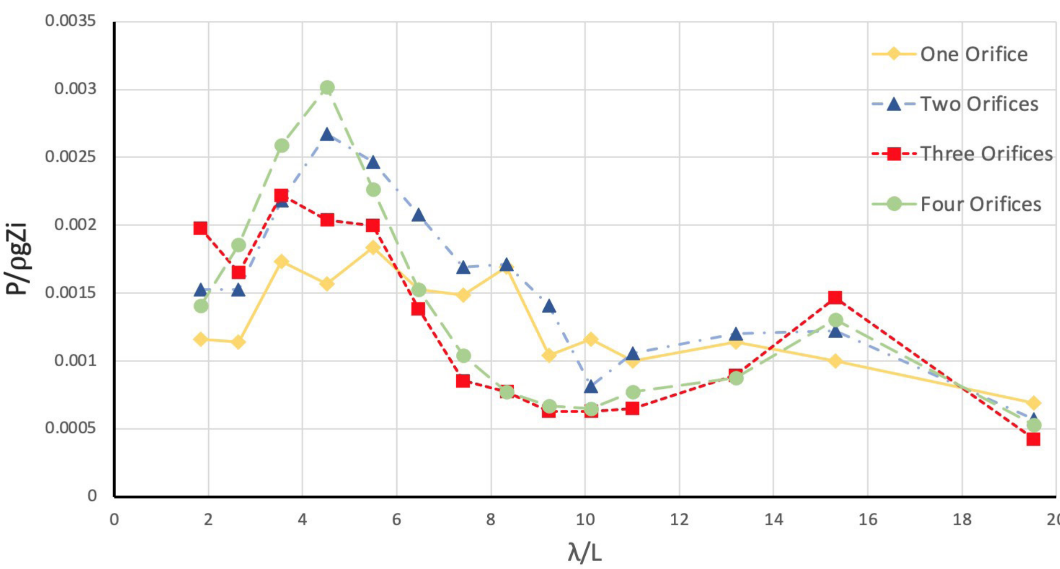

FIGURE 12. Amplitude of Inner Pressure for all top panels

FLOW RATE AT THE NOZZLE OUTLET

Similar to pressure, flow rate is also pivotal in measuring efficiency. As shown in Equation 5, flow rate affects the air energy, which later affects the efficiency output. Hence, an increase in flow rate will result in increased efficiency output. In this experiment, only the maximum flow rate was obtained when the wave reached the highest amplitude.

The flow rate at the nozzle outlet for all top panels was plotted in Figure 13. The measurement uncertainty for the flow rate data points, assuming a flow sensor accuracy of ±1% and a repeatability standard deviation of ±0.1 m^3/s, is approximately ±0.112 m^3/s. Based on the observations, all top panels showed a similar trend line between the flow rate and water elevation. The airflow rate for all top panels increased rapidly when λ/L = 1.8 to 5.0 with the exception of the top panel with 1 orifice where the airflow rate increased moderately. This is because the 1-orifice configuration had a very limited exit for air within the column, causing the air flowing near the corners of the column to become flow circulation. The high flow circulation within the column resulted in the loss of kinetic energy of the air particles, consequently causing the airflow to become lower. Once the flow rate for the 4-orifice top panel reached its peak, it began to decrease swiftly during λ/L = 6.0 to 9.0. Based on the graph plotted, it can be seen that the top panel with 4 orifices produced the highest air flow rate. It indicates that an increase in the number of orifices proved to improve the output performance due to the increase of the number of exits for the air to flow out. In contrast to the 1-orifice configuration, the 4-orifice configuration had four airflow exits that prompted less flow circulation within the column. This resulted in low kinetic energy and pressure loss, thus maintaining the high air flow rate caused by the pneumatic energy of the wave. Such results agree with Golijanek-Jedrzejczyk et al. (2022) who reported that multiple orifices have a higher flow rate than the standard central orifice because they are less responsive to flow disruptions.

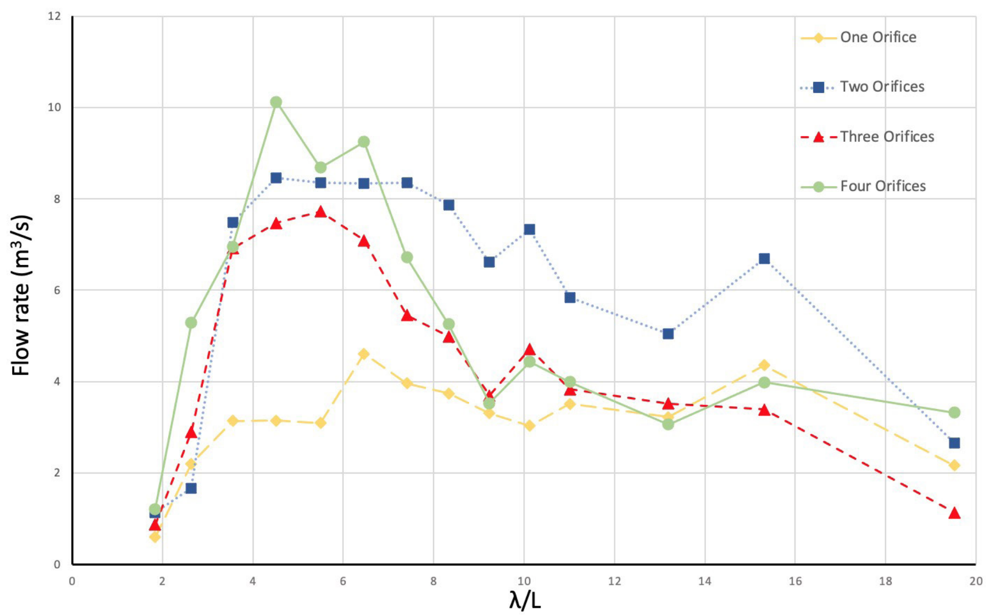

FIGURE 13. Air flow rate at the nozzle outlet

WAVE AND AIR ENERGY

Figure 14 displays the comparison of incident wave energy ($Ewave$) and pneumatic energy harvested from the water column chamber for all four top panels. It seems that the wave energy increased with the increase of λ/L. This happened since the wavelength (λ) contributes to energy; wavelength is one of the elements used in the calculation of group velocity (Cg). As shown in Figure 14 below, the top panel with 2 orifices had a maximum pneumatic energy of 3.5 kW compared to other top panels with 1 orifice, 3 orifices, and 4 orifices that recorded a maximum value of 1.9 kW, 1.09 kW, and 1.48 kW, respectively. For all top panels, the pneumatic energy was insignificant at λ/L = 11.0 onward. Although the top panel with 4 orifices had the highest pressure difference and flow rate, Figure 14 shows a different outcome where the top panel with 2 orifices produced the highest pneumatic energy. This is supported by a study from Zeng et al. [36] where 2 orifices have the lowest damping coefficient compared to other multiple orifices, which will increase the oscillation of the water inside the chamber and produce more energy. Another study by Jingbin et al. (2015) also reported that having 2 orifices will produce a higher nozzle discharge coefficient, which is the ratio of hydraulic energy discharged over initial hydraulic energy from incident flow condition. It is believed that a higher nozzle discharge coefficient will produce a higher hydraulic energy transfer, resulting in lesser energy loss.

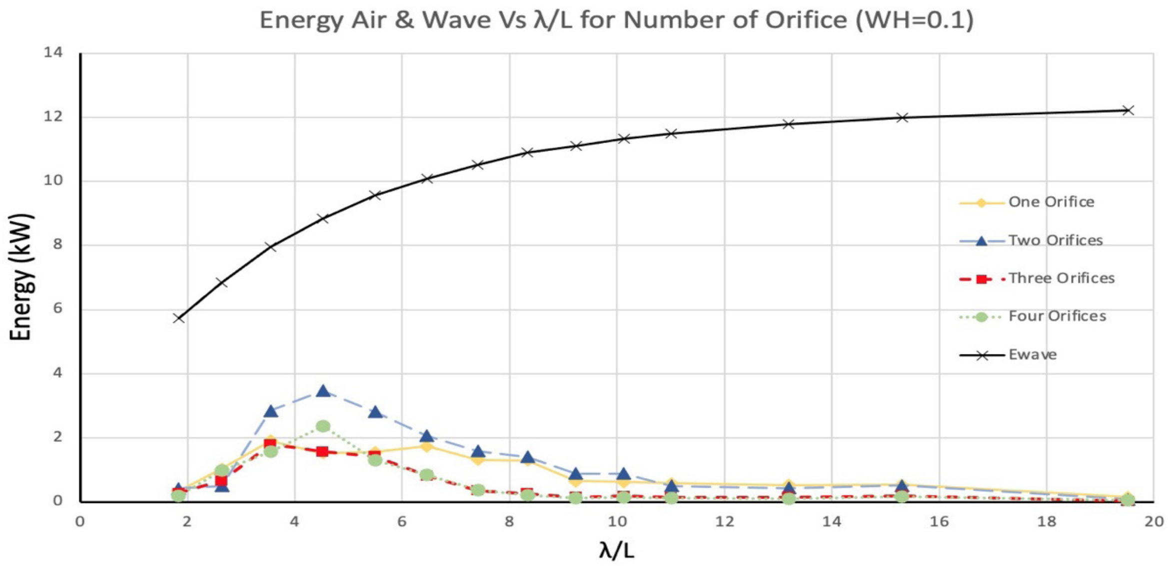

FIGURE 14. Wave and Air Energy for all top panels

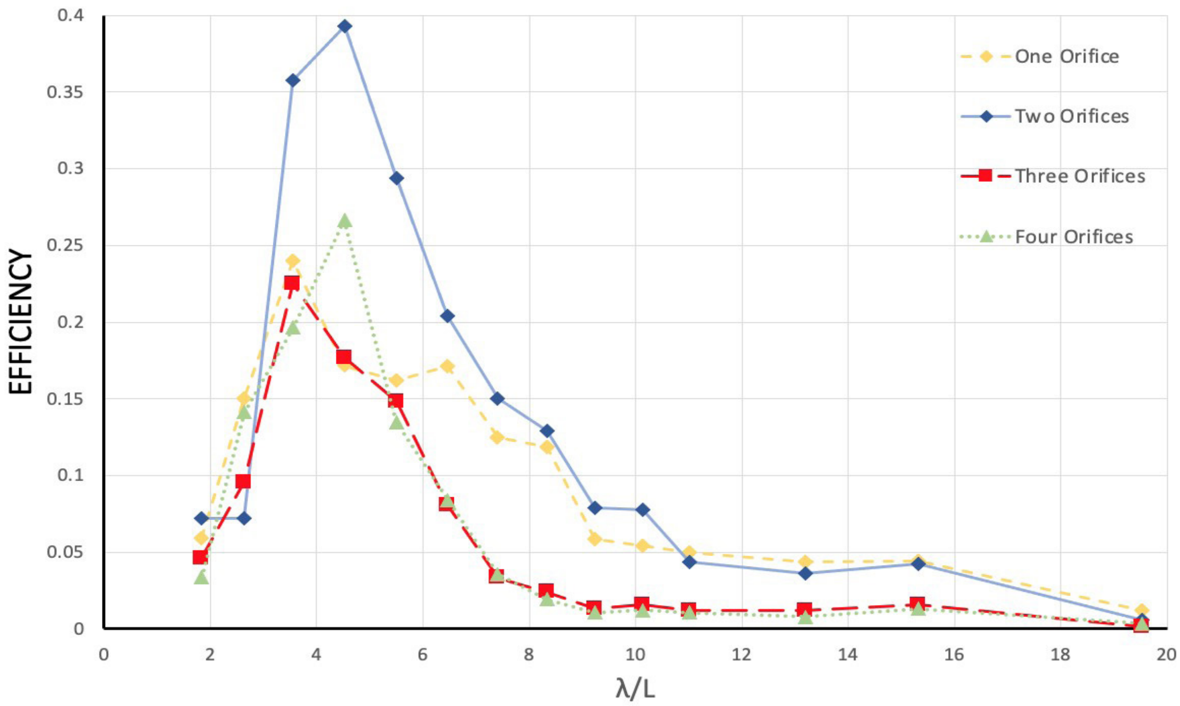

FIGURE 15. Efficiency of BBDB device for all top panels

PRIMARY CONVERSION EFFICIENCY OF BBDB DEVICE

Figure 15 shows the efficiency for all top panels with a wave height of 0.1 m. The top panel with 2 orifices outrun the other top panel by having the highest peak efficiency of 0.39. It increased expeditiously when $\lambda/L = 2.0$ to 5.0 and started to decrease moderately once it reached the peak. Meanwhile, both 1-orifice and 3-orifice top panels increased when $\lambda/L = 2.0$ to 4.0 and reached their peak efficiency of 0.23 and 0.22, respectively.

Whereas the efficiency for the 4-orifice top panel increased when $\lambda/L = 2.0$ and reached its peak at $\lambda/L = 4.5$ and a stall of efficiency from 0.27 to 0.08. Overall, it was observed that the efficiency of all top panels increased during the low λ/L conditions. The worst wave conditions were found to be between λ/L= 19.0 and 20.0, which plainly explained why such region should be avoided.

CONCLUSION

Our results showed that a single orifice BBDB device with a wave height of 0.05 m had the highest efficiency of 49% compared to other wave heights. The percentage difference of efficiency between the wave height of 0.05 m and 0.08 m as well as 0.05 m and 0.1 m were 54% and 51% respectively.

Regarding the performance of the BBDB device with multiple orifices, the results illustrated that the top panel with 2 orifices had the highest primary conversion efficiency of 39% and overpowered the other top panels with 1,3, and 4 orifices. Furthermore, the top panel with 2 orifices recorded a percentage difference of 41% as compared to the 1 orifice (baseline), followed by 44% with the 3-orifice top panel and 33% with the 4-orifice top panel. It was also found that the 3-orifice top panel recorded the highest percentage difference with the 2-orifice top panel. As for the top panel with 1 orifice, the wave height of 0.05 m produced the highest efficiency compared to other wave heights.

Furthermore, investigation of BBDB device using the 2D wave flume maker concluded that the top panel with 2 orifices had the highest primary conversion efficiency surpassing the efficiency of the baseline (1 orifice).

However, it should be noted that the data of this study were limited to primary conversion efficiency and since it was conducted in a 2D wave flume maker, the condition of the wave produced did not represent the actual wave conditions on the ocean. This stands as an area that can be improved in future studies by obtaining data that can enable the scope of secondary conversion efficiency and conducting similar experiment in a 3D wave basin that matches the actual wave conditions. The findings obtained from this study can serve as a reference for other researchers who are looking at the prospect of validating their simulation results. Finally, our findings can be extended to another research given that it uses a BBDB configuration.

ACKNOWLEDGEMENT

This research was supported by the research grant under Joint Research/Usage for Institute of Ocean Energy Saga University(IA009-UPNM/2023/SAGA UNIVERSITY/TK/01). The authors would also like to thank Universiti Pertahanan Nasional Malaysia (UPNM) for sponsoring the project through UPNM Postgraduate & Postdoctoral Research Grant (GPPP).

DECLARATION OF COMPETING INTEREST

None.

REFERENCES

Aderinto, T., & Li, H. 2018. Ocean wave energy converters: Status and challenges. Energies 11(5): 1250

Aiman, M. J., Ismail, N. I., Saad, M. R., Imai, Y., Nagata, S., Samion, M. K. H., Manan, E. A., & Rahman, M. R. A. 2020. Study on shape geometry of floating oscillating water column wave energy converter for low heave wave condition. *Journal of Advanced Research in Fluid Mechanics and Thermal Sciences* 70(2): 124-134.

Astariz, S., & Iglesias, G. 2015. The economics of wave energy: A review. *Renewable and Sustainable Energy Reviews* 45: 397-408.

Baanu, T. B., Mudgal, B. V., & Jalihal, P. 2014. Effect of duct extension on pneumatic efficiency of Backward Bent Duct Buoy (BBDB). *ISH Journal of Hydraulic Engineering* 20(2): 158-166.

Celik, A., & Altunkaynak, A. 2019. Experimental investigations on the performance of a fixed-oscillating water column type wave energy converter. *Energy* 167: 77-88.

Delmonte, N., Barater, D., Giuliani, F., Cova, P., & Buticchi, G. 2014. Oscillating water column power conversion: A technology review. In *2014 IEEE Energy Conversion Congress and Exposition (ECCE)* (pp. 1852-1859). IEEE.

Diaz, H., Sannasiraj, S. A., & Soares, C. G. 2018. Experimental study of behaviour and efficiency on a backward bent duct buoy. In *Advances in Renewable Energies Offshore* (pp. 203-210). Taylor & Francis Group.

Dincer, I., Rosen, M. A., & Khalid, F. 2018. ocean (marine) energy production. In *Comprehensive Energy Systems* (pp. 733-761). Elsevier.

Dolores, E. M., Jose, S. L., & Vicente, N. 2017. Classification of wave energy converters. Recent Advances in Petrochemical Science 2(1): RAPSCI.MS.ID.555576.

Doyle, S., & Aggidis, G. A. 2019. Development of multi-oscillating water columns as wave energy converters. *Renewable and Sustainable Energy Reviews* 107: 75-86.

Doyle, S., & Aggidis, G. A. 2020. Experimental investigation and performance comparison of a single OWC, array and M-OWC. *Renewable Energy* 146: 2729-2747.

Drew, B., Plummer, A. R., & Sahinkaya, M. N. 2009. A review of wave energy converter technology. *Proceedings of the Institution of Mechanical Engineers, Part A: Journal of Power and Energy* 223(8): 887-902.

Falcao, A. F. O. 2009. Wave energy utilization: A review of the technologies. *Renewable and Sustainable Energy Reviews* 14(3): 899-918.

Fusheng, L., Ruisheng, L., & Fengguan, Z. 2016. Microgrid and distributed generation. In *Microgrid Technology and Engineering Application* (pp. 1-18). Elsevier.

Golijanek-Jedrzejczyk, A., Mrowiec, A., Kleszcz, S., Hanus, R., Zych, M., & Jaszczur, M. 2022. A numerical and experimental analysis of multi-hole orifice in turbulent flow. *Measurement* 184: 109900.

Howe, D., & Nader, J. R. 2017. OWC WEC Integrated within a breakwater versus isolated: Experimental and numerical theoretical study. *International Journal of Marine Energy* 18: 25-43.

Husain, M. K. A., Zaki, N. I. M., Husin, S. M. C., Mukhlas, N. A., & Ahmad, S. Z. A. S. 2019. Integrated tidal marine turbine for power generation with coastal erosion breakwater. *International Journal of Civil Engineering and Technology* 10(2): 1-12.

Imai, Y., Toyota, K., Nagata, S., & Mamun, M. A. H. 2010. Duct extension effect on the primary conversion of a wave energy converter "backward bent duct buoy". Ocean Thermal Energy Conversion Laboratory, Faculty of Science and Technology, Saga University 15: 33-36.

Imai, Y., Toyota, K., Nagata, S., Setoguchi, T., Oda, J., Matsunaga, N., & Shimozono, T. 2008. An experimental study of negative drift force acting on a floating OWC Backward Bent Duct Buoy. In Proceedings of the ASME 2008 27th International Conference on Offshore Mechanics and Arctic Engineering (Vol. 3, pp. 871-879). ASME.

Jingbin, L., Gensheng, L., Zhongwei, H., & Xianzhi, S. A. 2015. A study about the effect of the structure parameters of the multi-orifices nozzle on nozzle discharge coefficient. In WJTA-IMCA Conference and Expo. November 2-4, New Orleans, Louisiana.

Joubert, J. R., Niekerk, J. L. V., Reinecke, J., & Meyer, I. 2013. *Wave Energy Converters (WECs)*. Centre for Renewable and Sustainable Energy Studies.

Kim, S., Koo, W., & Kim, M. 2015. Nonlinear time-domain NWT simulations for two types of a backward bent duct buoy (BBDB) compared with 2D wave-tank experiments. *Ocean Engineering* 95: 96-106.

Li, M., Wu, B., Jiang, C., & Zhang, Y. 2019. Effect of reciprocating and unidirectional airflow on primary conversion of a pentagonal Backward Bent Duct Buoy. *Applied Ocean Research* 82: 11-20.

Li, M., Wu, R., Wu, B., & Zhang, Y. 2019. Experimental study on conversion efficiency of a floating OWC pentagonal backward bent duct buoy wave energy converter. *China Ocean Engineering* 33(5): 525-533.

Lindroth, S., & Leijon, M. 2011. Offshore wave power measurements - A review. *Renewable and Sustainable Energy Reviews* 15(9): 4274-4285.

Macfarlane, G., Elhanafi, A., Fleming, A., & Leong, Z. 2017. Experimental and numerical investigations on the hydrodynamic performance of a floating-moored oscillating water column wave energy converter. *Applied Energy* 205: 1127-1141.

Murakami, T., Imai, Y., Nagata, S., Takao, M., & Setoguchi, T. 2016. Experimental research on primary and secondary conversion efficiencies in an oscillating water column-type wave energy converter. *Sustainability* 8(5): 487.

Pietra, L., Tello, M., Bhattacharjee, J., & Soares, C. G. 2012. Review and classification of wave energy converters. In *Maritime Engineering and Technology* (pp. 579-584). CRC Press.

Rezanejad, K., Soares, C. G., Lopez, I., & Carballo, R. 2017. Experimental and numerical investigation of the hydrodynamic performance of an oscillating water column wave energy converter. *Renewable Energy* 106: 1-16.

Toyota, K., Nagat, S., Imai, Y., Oda, J., & Setoguchi, T. 2010. Primary energy conversion characteristics of a floating OWC "Backward Bent Duct Buoy". In The International Society of Offshore and Polar Engineers.

Toyota, K., Nagata, S., Imai, Y., & Setogichi, T. 2008. Effects of hull shape primary conversion characteristics of a floating OWC "Backward Bent Duct Buoy". *Journal of Fluid Science and Technology* 3(3): 484-496.

Wu, B., Chen, T., Jiang, J., Li, G., Zhang, L., & Y. Ye. 2018. Economic assessment of wave power boat based on the performance of "Mighty Whale" and BBDB. *Renewable and Sustainable Energy Reviews* 92: 708-730.

Wu, B., Li, M., Wu, R., Chen, T., Zhang, Y., & Ye, Y. 2018. BBDB wave energy conversion technology and perspective in China. *Ocean Engineering* 163: 109-124.

Wu, B., Li, M., Wu, R., Zhang, Y., & Peng, W. 2017. Experimental study on primary efficiency of a new pentagonal backward bent duct buoy and assessment of prototypes. *Renewable Energy* 113: 90-99.

Wuebbles, D. J., & Jain, A. K. 2001. Concerns about climate change and the role of fossil fuel use. *Fuel Processing Technology* 71(1-3): 99-119.

Zeng, X., Zhang, L., Yu, F., & Zhou, J. 2017. The effect of an orifice plate with different orifice numbers and shapes on the damping characterisitcs of a dual-chamber air spring. *Journal of Vibroengineering* 19(4): 2375-2389.

Zhang, D., Li, W., & Lin, Y. 2009. Wave energy in China: Current status and perspectives. *Renewable Energy* 34(10): 2089-2092.